Indian Journal of Geo Marine Sciences
Vol. 54 (09), September 2025, pp. 441-451
DOI: 10.56042/ijms.v54i09.18333

# Uniqueness of discharge coefficient of sluice passage for tidal power plant: CFD modelling

J-S Jo*[,a] & K-S Kim[b]

[a]Faculty of Earth and Environmental Sciences, Kim Il Sung University, Ryongnam-Dong, Taesong-District, Pyongyang, Democratic People's Republic of Korea

[b]Department of Architectural Science, State Academy of Sciences, Ryonmot-Dong, Sosong-District, Pyongyang, Democratic People's Republic of Korea

*[E-mail: js.jo@ryongnamsan.edu.kp]

## Supplementary Text

### Theoretical analysis for uniqueness of discharge coefficient of sluice passage

From the steady-flow continuity (conservation of mass) equation[1], for any cross section of the sluice passage, we read $Q = A_iV_i$ = constant, ($i$ = 1, 2,…$n$) … (S1)

Where, $A_i$ is the area of the $i$th cross section and $V_i$ is the mean flow velocity at the $i$th cross section. The continuity equation (S1) is valid for both real and ideal flows.

On the other hand, the discharge coefficient ($C_d$) can also be expressed as $C_d = \frac{Q_{real}}{Q_{ideal}}$ (ref. 2) … (S2)

Where, $Q_{real}$ is the real flow rate and $Q_{ideal}$ is the ideal flow rate. From the steady-flow continuity, Eq. (S2) can be generalised for any cross section of the sluice passage as follows:

$$C_d = \frac{Q_{real\ ,i}}{Q_{ideal\ ,i}} = constant, (i = 1, 2,\dots n) \quad \dots \text{(S3)}$$

Where, $Q_{real,i}$ is the real flow rate at the $i$th cross section and $Q_{ideal,i}$ is the ideal flow rate at the $i$th cross section. Eq. (S3) has clearly shown that for steady incompressible flow with viscosity, the discharge coefficient of any one sluice passage is the only one (*i.e.*, the discharge coefficient determined at any cross section along the sluice passage is constant) and its value must be less than 1. This is another demonstration that, as described in the subsection "Discharge coefficient of sluice passages", the $C_d$ values at the throat and outlet sections are the same.

### Derivation of the discharge coefficient equation of the sluice passage

As shown in Figure S1, cross section 1-1 was taken at the free surface of the upstream flow, cross sections 2-2 and 3-3 at the throat and outlet of the sluice passage, and the bottom surface (section *O-O*) as the reference datum.

#### Discharge coefficient equation at throat (section 2-2)

The application of the Bernoulli equation and the energy–momentum method considering energy losses (EML)[3] between cross sections 1-1 (upstream) and 2-2 (throat) gives

$$h_1 + \frac{p_1}{\rho g} + \frac{V_1^2}{2g} = h_2 + \frac{p_2}{\rho g} + K\frac{V_2^2}{2g} + \Delta H_2 \quad \dots \text{(S4)}$$

Where, $h_1$ is the mean water level at the upstream, $p_1$ is the upstream pressure (= the atmospheric pressure, $p_{atm}$), $V_1$ is the mean velocity at the upstream, $\rho$ is the density of water, $g$ is the gravitational acceleration, $h_2$ is the mean water level at the throat (= the vertical distance from the reference datum to the passage ceiling), $p_2$ is the pressure at the throat ($\neq p_{atm}$), $V_2$ is the mean velocity at the throat, and $K = k + 1$ (where $k$ is the energy loss factor between the upstream and throat sections)[3], respectively. The term $\Delta H_2$ (= $\psi V_2^2$ / $2g$) is the total head loss (major head losses + minor head losses) between the upstream and throat sections, where $\psi$ is the combination of the loss coefficients (including the friction factors) of the sluice passage. That is, $\psi > 0$ for real flow.

Rearranging, Eq. (S4) becomes

$$h_1 + \frac{p_1}{\rho g} + \frac{V_1^2}{2g} = h_2 + \frac{p_2}{\rho g} + \frac{V_2^2}{2g} + k\frac{V_2^2}{2g} + \psi\frac{V_2^2}{2g} \quad \dots \text{(S5)}$$

Rearranging,

$$(1 + k + \psi)\frac{V_2^2}{2g} = h_1 + \frac{V_1^2}{2g} + \frac{p_1}{\rho g} - h_2 - \frac{p_2}{\rho g} \quad \dots \text{(S6)}$$

Rearranging,

$$V_2 = \frac{1}{\sqrt{1+k+\psi}}\sqrt{2g\Delta h_t} \quad \dots \text{(S7)}$$

Where, $\Delta h_t = \left(h_1 + \frac{p_1}{\rho g} + \frac{V_1^2}{2g}\right) - \left(h_2 + \frac{p_2}{\rho g}\right)$.

Thus, the discharge at the throat is

$$Q = V_2 A_t = \frac{A_t}{\sqrt{1+k+\psi}}\sqrt{2g\Delta h_t} = C_d A_t \sqrt{2g\Delta h_t} \quad \text{… (S8)}$$

Where, $A_t$ is the area of the throat section. As shown in Eq. (S8), the discharge coefficient $C_d$ at the throat section is

$$C_d = \frac{Q}{A_t\sqrt{2g\Delta h_t}} = \frac{1}{\sqrt{1+k+\psi}} < 1 \text{…(S9)}$$

**Discharge coefficient equation at outlet (section 3-3)**

The application of the Bernoulli equation and the EML between cross sections 1-1 and 3-3 (outlet) gives

$$h_1 + \frac{p_1}{\rho g} + \frac{V_1^2}{2g} = h_3 + \frac{p_3}{\rho g} + K\frac{V_3^2}{2g} + \Delta H_3 \quad \text{… (S10)}$$

Where, $h_3$ is the downstream mean water level immediately downstream from the passage, $p_3$ is the outlet pressure (= $p_{atm}$), and $V_3$ is the mean velocity at the outlet. The term $\Delta H_3 (= \psi\frac{V_3^2}{2g})$ is the total head loss (major head losses + minor head losses) between the upstream and outlet sections.

Noting that $p_1 = p_3 = p_{atm}$ and rearranging, Eq. (S10) becomes

$$h_1 + \frac{V_1^2}{2g} - h_3 = (1 + k + \psi)\frac{V_3^2}{2g} \quad \text{… (S11)}$$

Rearranging,

$$V_3 = \frac{1}{\sqrt{1+k+\psi}}\sqrt{2g\Delta h_e} \quad \text{… (S12)}$$

Where, $\Delta h_e = h_1 + \frac{V_1^2}{2g} - h_3$.

Thus, the discharge at the outlet is

$$Q = V_3 A_e = \frac{A_e}{\sqrt{1+k+\psi}}\sqrt{2g\Delta h_e} = C_d A_e \sqrt{2g\Delta h_e} \quad \text{… (S13)}$$

Where, $A_e$ is the area of the outlet section. As shown in Eq. (S13), the discharge coefficient $C_d$ at the outlet section is

$$C_d = \frac{Q}{A_e\sqrt{2g\Delta h_e}} = \frac{1}{\sqrt{1+k+\psi}} < 1 \quad \text{… (S14)}$$

## Supplementary References

1 Çengel Y A & Cimbala J M, *Fluid Mechanics: Fundamentals and Applications*, 1st edn, (McGraw-Hill, New York), 2006, pp. 929.

2 Li C & Mickan B, Humidity effect on the calibration of discharge coefficients of critical flow Venturi nozzles in a pVTt facility, *Flow Meas Instrum*, 46 (2015) 125–132. http://dx.doi.org/10.1016/j.flowmeasinst.2015.10.003

3 Habibzadeh A, Vatankhah A R & Rajaratnam N, Role of Energy Loss on Discharge Characteristics of Sluice Gates, *J Hydraul Eng*, 137 (9) (2011) 1079–1084. http://dx.doi.org/10.1061/(ASCE)HY.1943-7900.0000406

## Supplementary Tables:

Table S1 — Details about the mesh size in each direction, the number of mesh cells and the computational time for mesh resolutions

| Mesh | Passage type | Mesh size in each direction (m) $x$ | $y$ | $z$ | Number of mesh cells | Computational time (h) |
|---|---|---|---|---|---|---|
| Mesh-1 | Venturi | 1 | 1 | 1 | 263,376 | 0.41 |
| | Culvert | 1 | 1 | 1 | 263,376 | 0.39 |
| Mesh-2 | Venturi | 0.5 | 0.5 | 0.5 | 2,107,008 | 7.2 |
| | Culvert | 0.5 | 0.5 | 0.5 | 2,107,008 | 6.5 |
| Mesh-3 | Venturi | 0.25, 0.5 | 0.5 | 0.5 | 3,495,808 | 12.4 |
| | Culvert | 0.25, 0.5 | 0.5 | 0.5 | 3,495,808 | 12.2 |
| Mesh-4 | Venturi | 0.25, 0.5 | 0.5 | 0.25 | 6,991,616 | 32.9 |
| | Culvert | 0.25, 0.5 | 0.5 | 0.25 | 6,991,616 | 31.8 |
| Mesh-5 | Venturi | 0.25, 0.5 | 0.25 | 0.25 | 13,983,232 | 82.3 |
| | Culvert | 0.25, 0.5 | 0.25 | 0.25 | 13,983,232 | 81.8 |

Table S2 — Comparison of measured and simulated $\Delta h_e$ for different mesh resolutions, at $Q$ = 600 $m^3/s$

| Mesh | Passage type | Simulated $\Delta h_e$ (m) | Measured $\Delta h_e$ (m) | Relative error (%) |
|---|---|---|---|---|
| Mesh-1 | Venturi | 0.852 | 0.55 | 54.909 |
| | Culvert | 0.228 | 0.42 | 45.714 |
| Mesh-2 | Venturi | 0.631 | 0.55 | 14.727 |
| | Culvert | 0.476 | 0.42 | 13.333 |
| Mesh-3 | Venturi | 0.582 | 0.55 | 5.818 |
| | Culvert | 0.444 | 0.42 | 5.714 |
| Mesh-4 | Venturi | 0.579 | 0.55 | 5.273 |
| | Culvert | 0.398 | 0.42 | 5.238 |
| Mesh-5 | Venturi | 0.575 | 0.55 | 4.545 |
| | Culvert | 0.438 | 0.42 | 4.286 |

Table S3 — Simulated head difference, $\Delta h_e$ (m), using different turbulence models, against the measured value at $Q$ = 600 $m^3/s$

| Passage type | Measured $\Delta h_e$ (m) | Simulated $\Delta h_e$ (m) | | | Relative error (%) | | |
|---|---|---|---|---|---|---|---|
| | | standard $k-\varepsilon$ | $k-\omega$ | RNG $k-\varepsilon$ | standard $k-\varepsilon$ | $k-\omega$ | RNG $k-\varepsilon$ |
| Venturi | 0.55 | 0.603 | 0.595 | 0.582 | 9.636 | 8.182 | 5.818 |
| Culvert | 0.42 | 0.381 | 0.453 | 0.444 | 9.286 | 7.857 | 5.714 |

Table S4 — Flow conditions in the laboratory model (venturi-type passage)

| $Q$ ($m^3/s$) | $V_u$ (m/s) | Re (-) | Fr (-) |
|---|---|---|---|
| 0.0296 | 0.19 | 73719.86 | 0.093 |
| 0.0395 | 0.25 | 98376.17 | 0.125 |
| 0.0494 | 0.31 | 123032.48 | 0.156 |
| 0.0593 | 0.37 | 147688.78 | 0.187 |

## Supplementary Figures:

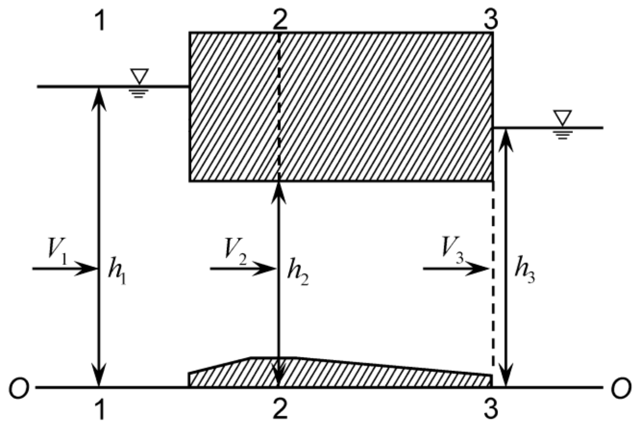


Fig. S1 — Schematic sluice passage model for deriving the discharge coefficient equation